JACS
JOURNAL OF THE AMERICAN CHEMICAL SOCIETY

Article

pubs.acs.org/JACS

Benzimidazole-Based Ratiometric Two-Photon Fluorescent Probes for Acidic pH in Live Cells and Tissues

Hyung Joong Kim,[†] Cheol Ho Heo,[†] and Hwan Myung Kim*

Division of Energy Systems Research, Ajou University, Suwon 443-749, Korea

Supporting Information

ABSTRACT: Many aspects of cell metabolism are controlled by acidic pH. We report a new family of small molecule and ratiometric two photon (TP) probes derived from benzimidazole (BH1−3 and BH1L) for monitoring acidic pH values. These probes are characterized by a strong two-photon excited fluorescence, a marked blue-to-green emission color change in response to pH, pK_a values ranging from 4.9 to 6.1, a distinctive isoemissive point, negligible cytotoxicity, and high photostability, thereby allowing quantitative analysis of acidic pH. Moreover, we show that BH1L optimized as a lysosomal-targeted probe allows for direct, real-time estimation of the pH values inside lysosomal compartments in live cells as well as in living mouse brain tissues through the use of two-photon microscopy. These findings demonstrate that these probes will find useful applications in biomedical research.

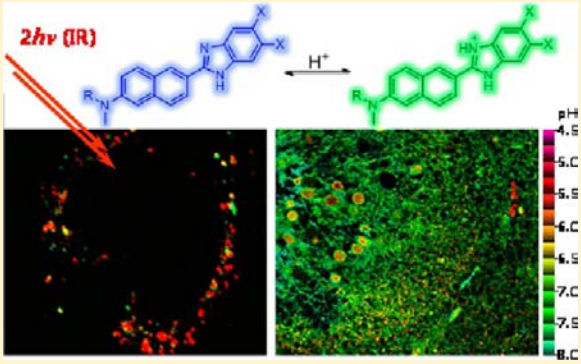

INTRODUCTION

Many cellular metabolic pathways are regulated by pH values in the acidic range, including endocytic processes, signaling, apoptosis, and defense. An acidic environment can serve to activate enzyme functions and protein degradation.[1] In eukaryotic cells, acidic organelles including lysosomes (pH 4.5−5.5) and endosomes (pH 4.5−6.8) contain numerous enzymes and secretory proteins exhibiting a variety of activities and functions.[2] In contrast, abnormal pH values in these organelles could be related to cellular dysfunctions, which are associated with many diseases such as cancer and neurodegenerative disorders.[3] To extend our understanding of the roles of acidic environments in biology and pathology, it is crucial to monitor subcellular pH values and their fluctuation at the cell, tissue, and organism level.

Molecular imaging with fluorescence microscopy has become an indispensable tool in the study of pH, with respect to spatial-temporal patterns. Two main classes of pH sensitive fluorescent probes have been developed. The first is a turn-on probe based on a photoinduced electron transfer system.[4] The second is a ratiometric probe based on a spectral shift in the absorption and/or emission during proton binding.[5,6] Of these two types of probes, the emission ratiometric probes have been mostly used for quantitative analysis, because a turn-on response within a single detection window can vary depending on the experimental conditions such as incident laser power and probe distribution. To monitor acidic pH, green fluorescent proteins (GFPs) and small molecule probes (such as LysoSensor DND-160 and fluorescein derivatives) have been widely used as ratiometric one-photon probes.[5b,7] GFPs, however, become denatured in an acidic environment (pH < 5).[8] Small molecule probes have the advantage of not requiring transfection as do its protein counterparts. In addition, use of these probes with one-photon microscopy requires a rather short excitation wavelength, which limits their application in live tissue imaging owing to the shortcomings of shallow penetration depth (<100 μm), photobleaching, photodamage, and cellular autofluorescence.

An attractive approach to the detection of pH values in live cells and tissues is ratiometric imaging with two-photon microscopy (TPM). TPM, which employs two near-infrared photons as the excitation source, offers a number of advantages including greater penetration depth (>500 μm), localization of excitation, and longer observation times.[9,10] Combined with appropriate TP probes, TPM can visualize biological events within live cells and intact tissues with minimum interference from background emissions and minimum photodamage.

Recently, a ratiometric TP probe derived from 2-aminofluorene has been reported for assessing near neutral pH (pK_a = 7.0) in cells.[11] A small molecule TP probe as an analogue of DND-160 (NP1, pK_a = 4.4) has also been reported to estimate acidic pH in live tissues by ratiometric TPM imaging.[12] However, NP1, possessing pyridine as its proton binding site, has low fluorescent quantum yield (<0.1), especially under acidic conditions. Moreover, for precisely assessing the acidic environments, there is a critical need for the TP probes with pK_a values in the range of 4.5−6.5.[5a] In addition, to detect the pH inside a specific organelle, one must find a pH sensitive dye that can be easily modified by introducing the targeting moiety.

Received: September 27, 2013
Published: November 6, 2013

   dx.doi.org/10.1021/ja409971k | J. Am. Chem. Soc. 2013, 135, 17969−17977

Scheme 1. (a) Design Strategy of BH Series;(b) Structures of BH1−3, BH1L, and P1

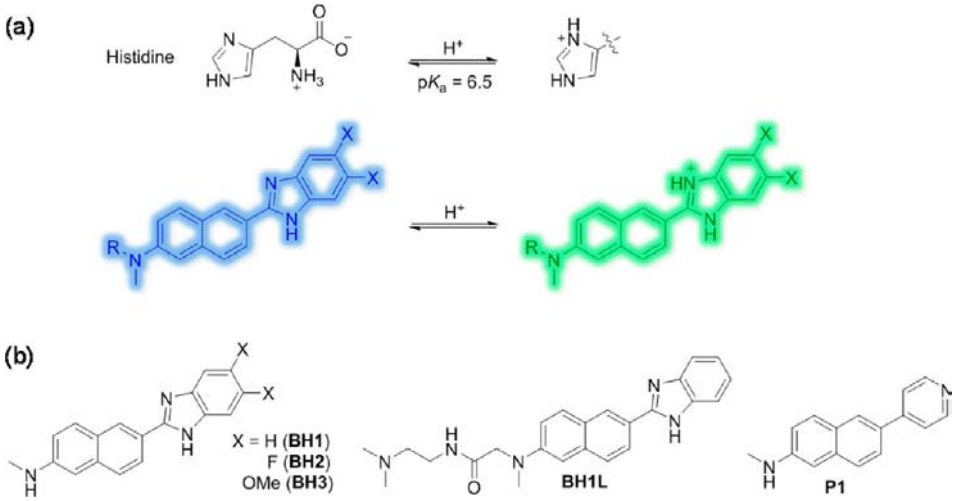

Table 1. Photophysical Data for BH Series and P1[a]

probe	pH	$\lambda_{max}^{(1)}$ (10^{-4} ε)[b]	λ_{max}^{fl}[c]	Φ[d]	pK_a[e]	$\lambda_{max}^{(2)}$[f]	δ[g]	$\Phi\delta$
BH1	pH 3.5	368(1.94)	494	0.76	5.91 (5.89)	750	185	140
	pH 7.2	337(2.53)	455	1.00		740	40	40
	pH 10	337(2.76)	453	1.00		740	35	35
BH2	pH 3.5	370(1.96)	499	0.76	4.92 (4.88)	750	200	155
	pH 7.2	339(2.84)	457	1.00		740	50	50
	pH 10	338(2.84)	457	1.00		740	45	45
BH3	pH 3.5	365(2.25)	488	0.79	6.11 (6.10)	750	80	65
	pH 7.2	345(2.98)	451	0.93		750	20	20
	pH 10	345(2.96)	448	0.94		750	20	20
BH1L	pH 3.5	368(2.98)	490	0.72	5.82 (5.86)	750	390	280
	pH 7.2	341(3.03)	448	1.00		750	95	95
	pH 10	341(3.05)	446	1.00		750	80	80
P1	pH 3.5	395(1.61)	nd[h]	nd[h]	nd[h]	nd[h]	nd[h]	nd[h]
	pH 7.2	333(1.52)	485	0.008		nd[h]	nd[h]	nd[h]
	pH 10	330(1.67)	492	0.009		nd[h]	nd[h]	nd[h]

[a]All the measurement were performed in universal buffer solution (0.1 M citric acid, 0.1 M KH_2PO_4, 0.1 M $Na_2B_4O_7$, 0.1 M tris(hydroxymethyl)aminomethane, 0.1 M KCl). [b]λ_{max} of the one-photon absorption spectra in nm. The numbers in parentheses are molar extinction coefficients in $M^{-1}cm^{-1}$. [c]λ_{max} of the one-photon emission spectra in nm. [d]Fluorescence quantum yield. [e]pK_a values measured by one-photon mode. The values in parentheses are measured by two-photon mode. [f]λ_{max} of the two-photon excitation spectra in nm. [g]Two-photon action cross-section in 10^{-50} cm^4 s/photon (GM units). [h]Not determined. The one- and two-photon excited fluorescence signals were too small to determine the values.

Toward this end, we report a series of ratiometric TP probes for acidic pH derived from benzimidazole (BH1−3, Scheme 1) that can quantitatively analyze subcellular pH values. Moreover, we present a lysosomal-targeted probe (BH1L, Scheme 1) that allows for direct, real-time estimation of the pH values within lysosomal compartments in live cells and living tissues using TPM.

RESULTS AND DISCUSSION

Design and Preparation of BH Series. Histidine is an essential amino acid containing imidazole, which is a titratable group that contributes to the buffering capacity of biological systems (Scheme 1).[13] Benzimidazole is a derivative of imidazole, which has an ideal pK_a value (pK_a ≈ 5.5) for acidic organelles.[14] We therefore designed a small molecule probe possessing benzimidazole substituents as a proton binding site at the 6-position of 2-aminonaphthalene (BH1−3). We undertook these studies with two aims in mind. First, the ratiometric detection of pH would be possible if protonation at the nitrogen in the benzimidazole resulted in a red-shifted emission. In addition, its own pK_a value can be easily modified by introducing electron donating or electron withdrawing groups on the benzimidazole. Second, we have utilized a naphthalene core because similar derivatives showed a significant TP action cross section ($\Phi\delta_{TPA}$) which is the product of the fluorescence quantum yield (Φ) and the two-photon absorption cross sections (δ_{TPA}), which have been successfully applied to TPM in live tissues and living mice.[15]

Compounds BH1−3 were synthesized by condensation of the 6-formyl-2-(*N*-methylamino)naphthalene with *o*-phenylenediamine derivatives. The detailed synthetic procedure is described in the Supporting Information. BH1L was designed by introducing the tertiary amine substituent (pK_a ≈ 10) to BH1 through an amide linkage, with the expectation that BH1L will accumulate in acidic organelles as the protonated form.[5b,16] We also prepared a counterpart (P1) containing pyridine (pK_a ≈ 5.0) as the protonation site because these compounds are commonly used as fluorescent probes for acidic pH.[5b,12,17]

dx.doi.org/10.1021/ja409971k | J. Am. Chem. Soc. 2013, 135, 17969−17977

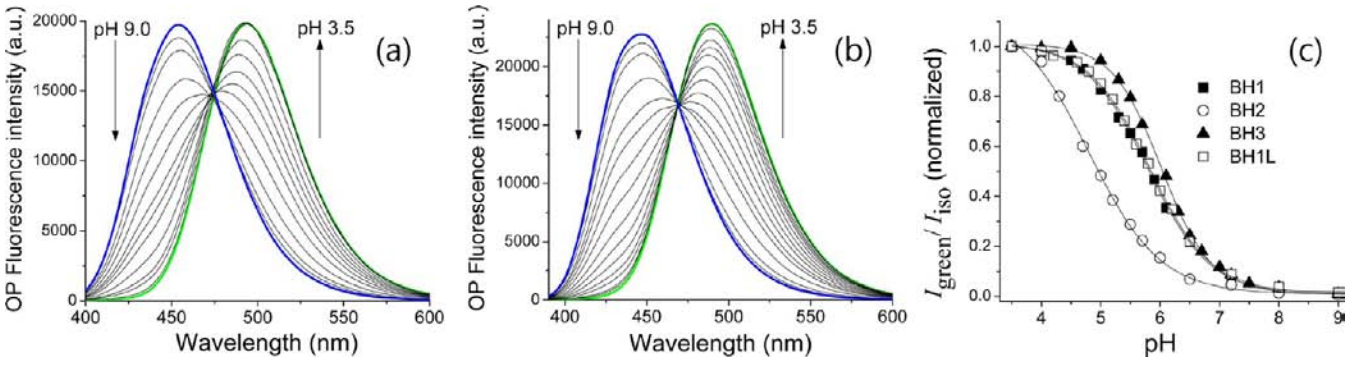

Figure 1. (a and b) The changes in one-photon fluorescence spectra of (a) BH1 and (b) BH1L with pH in universal buffer. (c) Plots of I_{green}/I_{iso} versus pH for BH1−3 and BH1L determined by one-photon mode. The excitation wavelength is 360 nm.

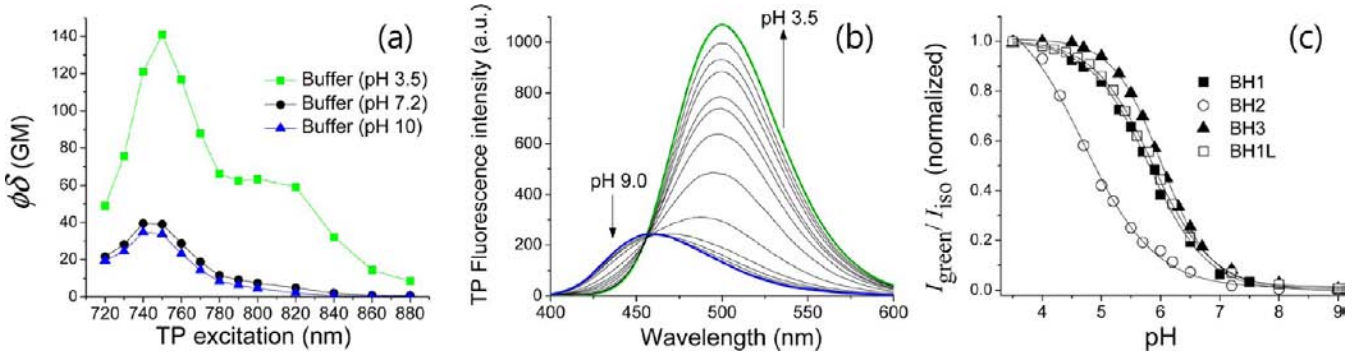

Figure 2. (a) Two-photon action ($\delta\Phi$) spectra of BH1 in universal buffer solutions at pH 3.5, 7.2, and 10, respectively. (b) The changes in two-photon excited fluorescence spectra of BH1 with pH in universal buffer. (c) Plots of I_{green}/I_{iso} versus pH for BH1−3 and BH1L determined by two-photon mode. Data in (c) is normalized at the maximum I_{green}/I_{iso}. The excitation wavelength for two-photon mode is 740 nm.

Photophysical Properties of BH Series in One-Photon Mode. The solubility of BH1 in universal buffer solution (pH 7.2) was 4 μM, which is 2-times more soluble than BH2 (2 μM), but less than half as soluble as BH3 (>10 μM). The solubility values of BH1L and P1 were >10 and 2 μM, respectively (Figure S1). Under these conditions (pH 7.2), BH1 has an absorption maximum (λ_{abs}) at 337 nm and a fluorescence emission maximum (λ_{fl}) at 455 nm with a large Stokes shift of 118 nm (Table 1). Under basic condition (pH 10), nearly identical results were observed as at pH 7.2 (Table 1). On the other hand, when the pH was changed from neutral (7.2) to acidic (3.5), the λ_{abs} and λ_{fl} of BH1 were shifted to a longer wavelength at 368 and 494 nm, respectively (Figure 1a and Table 1). These spectral red-shifts might be a result of protonation at the benzimidazolyl nitrogen (BH1-H$^+$), thereby enhancing the intramolecular charge transfer (ICT).[18] It is worth noting that both of BH1 (Φ = 1.00) and BH1-H$^+$ (Φ = 0.76) show the largest fluorescent quantum yield reported to date among pH probes in physiological buffer. Further, a sharp isoemission point at 474 nm was observed between two fully resolved λ_{fl} at 455 and 494 nm (Figure 1a). Similar spectral results were observed for BH2 and BH3 (Table 1 and Figure S2). As expected, these spectral data for BH1L was nearly identical to those of BH1 (Figure 1b and Table 1). In contrast, P1 showed negligible fluorescence (Φ = 0.008) in pH 7.2 and no fluorescence in pH 3.5, while the λ_{abs} gradually shifted from 333 to 395 nm (Table 1 and Figure S3). Consequently, the BH series showed a marked blue-to-green emission color change in response to a change in pH from neutral to acidic and the largest Φ in physiological buffer.

pK_a Values of BH Series. The pK_a of the conjugate acids of BH1−3 were derived from the titration curve of emission ratios (I_{green}/I_{iso}) at isoemission point (I_{iso}) and 500−550 nm (I_{green}). The pK_a values ranging from 4.92 to 6.11 (Table 1) indicated that the BH compounds are suitable for assessing acidic media (Figure 1c and Table 1). Their pK_a shifts are likely due to the electron withdrawing (F for BH2) or donating groups (OMe for BH3) within the protonating site. Here again, the pK_a value for BH1L was almost identical to that of BH1 (Table 1).

Photophysical Properties of BH Series in Two-Photon Mode. We then evaluated the abilities of the BH series to determine the pH value in a TP mode. The TP action spectra ($\Phi\delta$) of BH1 at pH 7.2 and 3.5 indicated $\Phi\delta_{max}$ values of 40 and 140 GM, respectively (Figure 2a and Table 1). The 3.5-fold larger $\Phi\delta_{max}$ value of BH1-H$^+$, possessing a stronger electron-withdrawing group than that of BH1, can be attributed to the enhanced ICT between the donor and acceptor.[18] Similar results were obtained for BH2 and its protonated form, while BH3 displayed approximately 2-fold smaller $\Phi\delta_{max}$ values than that of BH1 (Table 1 and Figure S4). Interestingly, both BH1L and protonated form showed 2-fold larger δ_{max} values than those of BH1 (Table 1 and Figure S4). Although the origin is unclear, this increment might be due to the peripheral group. Moreover, the characterizations of the TP excited fluorescence (TPEF) spectra of BH1 with pH exhibited similar behaviors to those obtained from the one-photon process, in terms of $\Delta\lambda_{fl} \approx$ 50 nm, a distinctive isoemissive point, and pK_a values (Figure 2b,c and Table 1). On the other hand, TP emission ratio (I_{green}/I_{iso}) increased by 10-fold as the pH value was changed from 7.2 to 3.5, and this value was >2-fold larger than that obtained from the one-photon process. Because the $\Phi\delta_{max}$

dx.doi.org/10.1021/ja409971k | J. Am. Chem. Soc. 2013, 135, 17969−17977

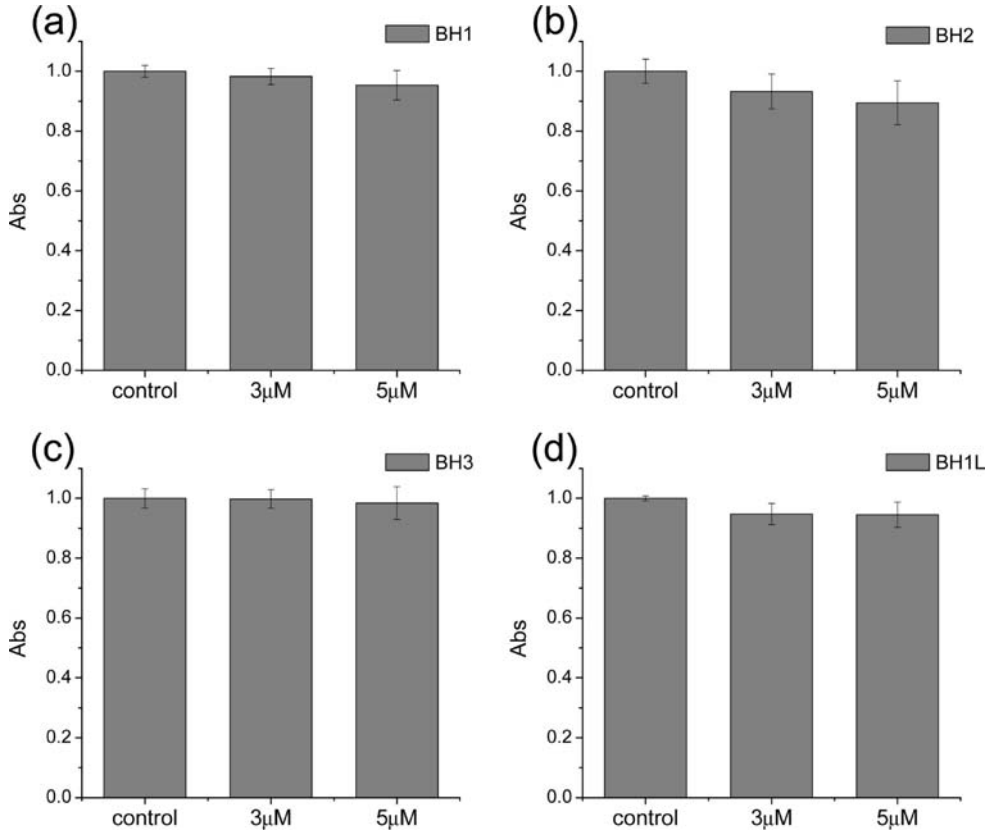

Figure 3. Viability of HeLa cells in the presence of (a) BH1, (b) BH2, (c) BH3, and (d) BH1L as measured by using MTS assay. The cells were incubated with probe for 24 h.

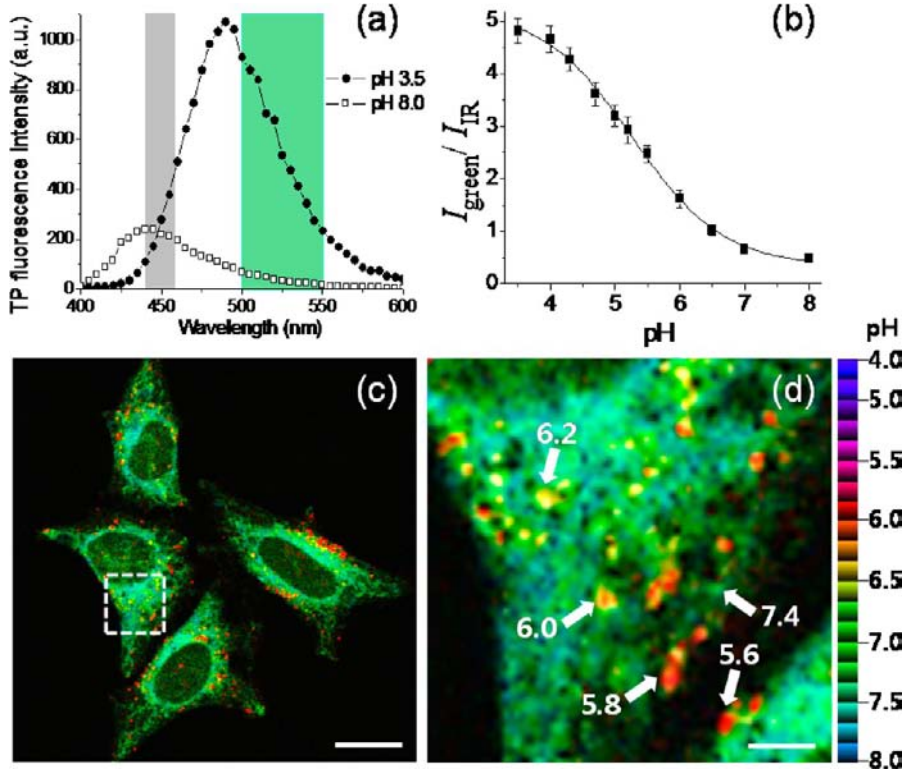

Figure 4. (a) Two-photon excited fluorescence spectra of ionophore-treated HeLa cells labeled with 3 μM BH1 at pH 3.5 and pH 8.0. (b) Two-photon I_{green}/I_{IR} titration with pH in HeLa cells. (c) Pseudocolored ratiometric TPM images (I_{green}/I_{IR}) of HeLa cells incubated with 3 μM BH1. (d) Higher magnification of boxed areas in (c). The numbers in (d) are the estimated pH values at the region of interest indicated by white arrows. Excitation wavelength is 740 nm. Scale bars are (c) 30 μm and (d) 5 μm. Cells shown are representative images from replicate experiments (n = 10).

dx.doi.org/10.1021/ja409971k | J. Am. Chem. Soc. 2013, 135, 17969−17977

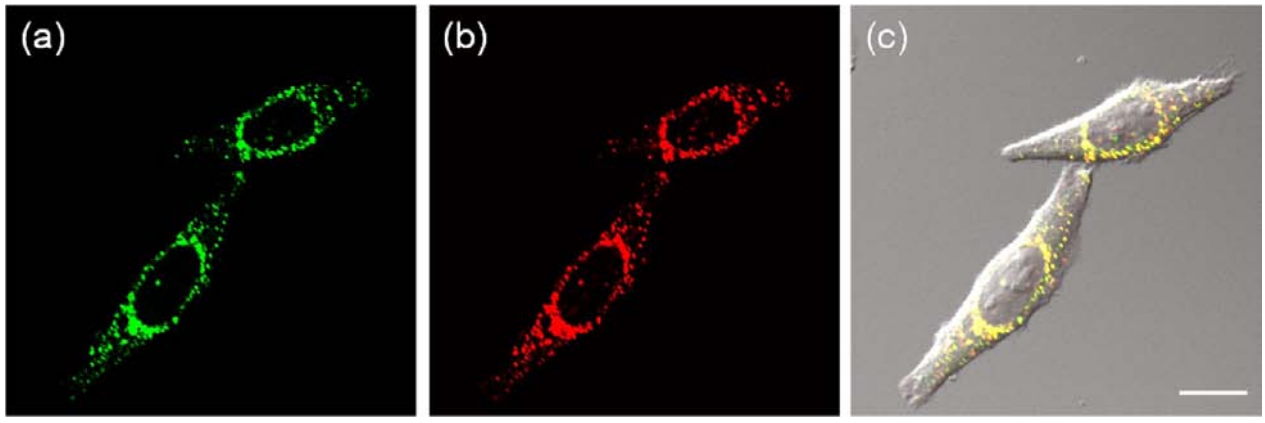

Figure 5. (a) TPM and (b) OPM images of HeLa cells co-labeled with BH1L and LysoTracker Red. (c) Merged image from (a), (b), and the corresponding contrast image. Excitation wavelengths for TPM and OPM are 740 and 543 nm, respectively. Scale bar = 20 μm. Cells shown are representative images from replicate experiments (n = 10).

value of the protonated form of BH1 is >3-fold larger than that of deprotonated form (Figure 2a), this result can be attributed to the larger TPEF enhancement at 500−550 nm (I_{green}) in comparison with the one-photon process (Figures 1a and 2b). Similar results were observed for BH2, BH3 and BH1L (Figure S2).

The TPM images of HeLa cells labeled with the BH series probes were bright (Figures S5), presumably because of the significant $\Phi\delta_{max}$ values, whereas the images of P1-labeled HeLa cells showed no TPEF (Figure S6). In addition, BH series show high photostability as revealed by the negligible changes in the TPEF intensity in the HeLa cells over 60 min (Figure S5) and negligible cytotoxicity as measured by a MTS assay (Figure 3). These outcomes establish that the BH series can serve as ratiometric TP probes that can estimate the pH value in acidic environments through the use of TPM with reasonable accuracy, and minimum interference from photostability and cytotoxicity issues.

Live Cell Calibration with BH1. We next sought to utilize BH1 as a TP probe to determine the pH value in cells with TPM. Using 740 nm TP excitation in scanning lambda ($xy\lambda$) mode, ionophore-treated HeLa cells labeled with BH1 at pH 8.0 and pH 3.5 emitted TPEF spectra with λ_{fl} of 445 and 490 nm, respectively (Figure 4a). Importantly, they are nearly identical to those of BH1 in the buffer solution (Figure 2b), except that both λ_{fl} are slightly blue-shifted within 10 nm. Since the emission spectra of BH1 showed gradual red shifts with increasing solvent polarity (Figure S7 and Table S1), this observation indicates that the probe environment in cells is rather homogeneous and slightly more hydrophobic than in buffer, which is similar to EtOH:buffer (1:1). This outcome allowed ratiometric imaging (I_{green}/I_{IR}) for intracellular pH by using 440−460 nm (I_{IR}) as an internal reference window and 500−550 nm (I_{green}) as a pH recognition window (Figure 4a). Moreover, a pH calibration curve was generated by I_{green}/I_{IR} of ionophore-treated and BH1-labeled HeLa cells (Figure 4b). The pK_a value is of 5.34 ± 0.04, which is slightly lower than that measured in buffer (5.91), as previously reported.[6e] Furthermore, the plots of I_{green}/I_{IR} versus the pH value are linear at pH 4.0−7.0, indicating that BH1 is suitable to determine pH values in this range (Figure 4b). More importantly, the ratiometric TPM image (I_{green}/I_{IR}) of HeLa cells labeled with BH1 revealed the various pH values ranging from 5.6 to 7.4 throughout the subcellular compartments (Figures 4d and S8).

Estimation of Lysosomal pH Values with BH1L. We then sought to utilize BH1L as a lysosome-targeted TP probe to estimate the pH values. To assess whether BH1L can selectively locate in lysosomes, the HeLa cells were co-labeled with BH1L and Lysotracker Red DND-99 (LTR), a well-known one-photon probe for the lysosome. The TPM and OPM images overlapped well with the Pearson's colocalization coefficient = 0.95 (Figure 5). Moreover, ionophore-treated HeLa cells labeled with BH1L at pH 8.0 and pH 3.5 emitted TPEF spectra with λ_{fl} of 445 and 485 nm, respectively (Figure 6a), which are nearly identical to the values obtained from buffer (Figure S2).[16] Consistently, the pK_a value derived from ionophore-treated and BH1L-labeled HeLa cells was of 5.63 ± 0.08, a result similar to that measured in buffer (Figure 6b).

The ratiometric TPM image (I_{green}/I_{IR}) of BH1L-labeled HeLa cells showed the various pH values in the lysosomal compartment (Figure 6). It is worth noting that the individual pH values of individual spots ranging from 4.6 to 5.9 was clearly visualized (Figure S9) along with the average value of 5.1 ± 0.2 (n = 25). We next monitored the pH changes inside of lysosomes in real-time. Upon addition of 5 mM NH_4Cl, a weak base that increase intralysosomal pH,[19] the pH values began to rise in 2.3 min and reached a maximum value of 6.5−6.7 after 4 min (Figure 6g and S10). Most importantly, the small fluctuation in 0.1 pH unit was clearly visualized with their active movements (Figure S10). Therefore, BH1L is clearly capable of monitoring the change of intralysosomal pH values along with their transportation in live cells.

Mapping the pH Values in Live Rat Brain Tissues. We further investigated the utility of BH1L in a fresh slice of rat hippocampus, a region of the brain that is important for learning and memory. Because the structure of the brain tissue is known to be nonhomogeneous, we accumulated 120 ratiometric TPM images (I_{green}/I_{IR}) at 90−180 μm depth (Figure S11). They showed the overall pH distribution in the regions of CA1, CA3 and the dentate gyrus (DG) (Figure 7a), in which the acidic pH is more distributed in the DG than in CA regions. It has been well established that the DG region differs from CA regions, in particular, the cell type and the functions including neurogenesis and gene expression.[20] The abundance of acidic pH in the DG might be linked to the metabolic processes in this region, thus pointing to the need for

dx.doi.org/10.1021/ja409971k | J. Am. Chem. Soc. 2013, 135, 17969−17977

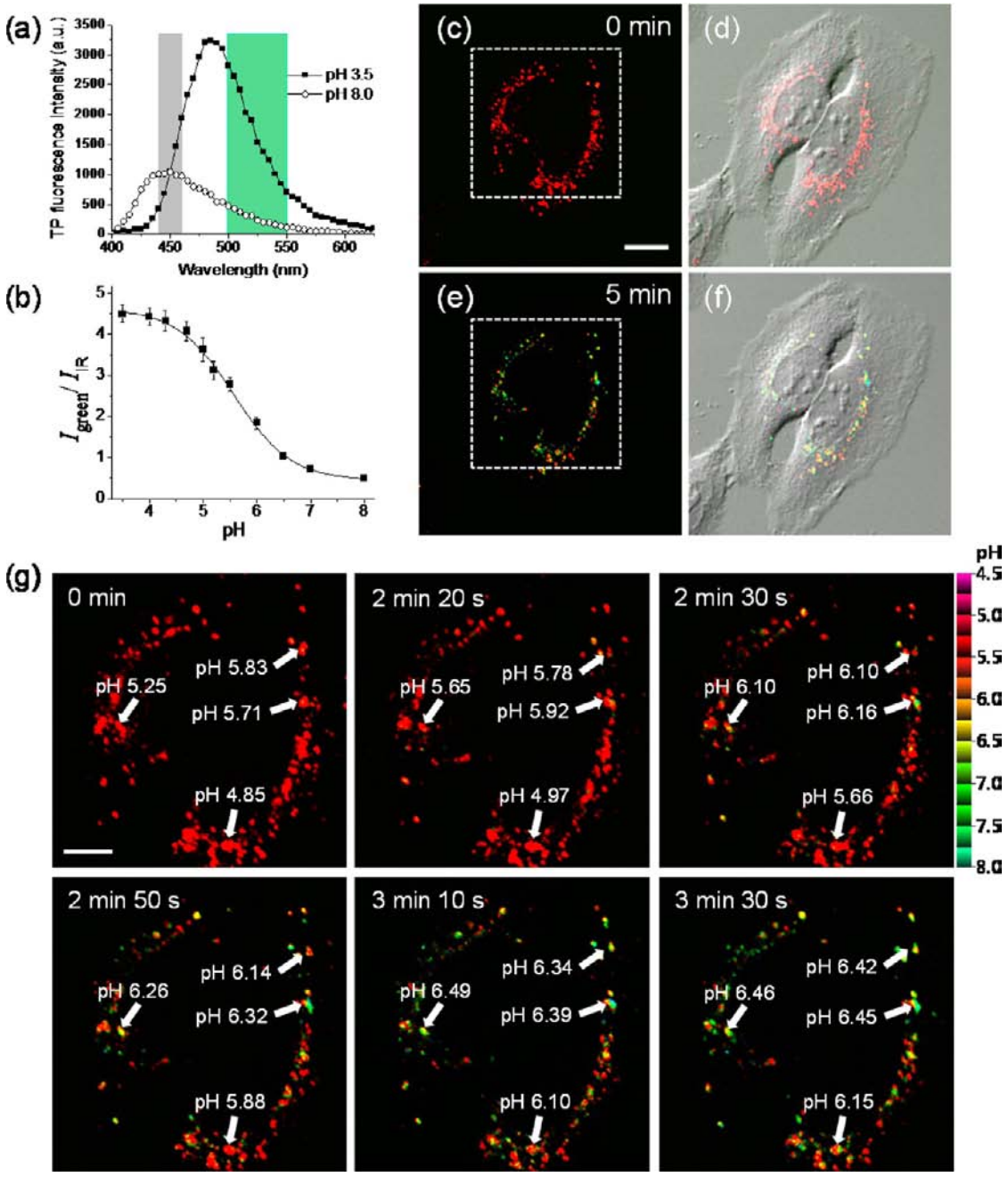

Figure 6. (a) Two-photon excited fluorescence spectra of ionophore-treated HeLa cells labeled with 3 μM BH1L at pH 3.5 and pH 8.0. (b) Two-photon I_{green}/I_{IR} titration with pH in ionophore-treated and BH1L-labeled HeLa cells. (c and e) Pseudocolored ratiometric TPM images (I_{green}/I_{IR}) of HeLa cells incubated with 3 μM BH1L before (c) and after (5 min) (e) addition of 5 mM NH_4Cl to the imaging solution, and (d and f) merged images with the corresponding DIC images. (g) Enlargement of a white box in (c) showing the changes of pH with time. The numbers in (g) are the estimated pH values at the region of interest indicated by white arrows. Excitation wavelength is 740 nm. Scale bars are (c) 20 μm and (g) 8 μm. Cells shown are representative images from replicate experiments (n = 25).

future studies to investigate its biological function. Moreover, the image at a higher magnification clearly showed the acidic compartments in the individual cells in the DG at a depth of about 100 μm (Figures 7b and S12). A similar result was observed for BH1-labeled tissue (Figure 7c,d), except that the acidic spots in Figure 7a are clearer than those stained with BH1. The combined results confirm that BH1L is clearly capable of estimating the pH values of subcellular acidic compartments in live cells and living tissues by using TPM.

■ CONCLUDING REMARKS

In conclusion, we have developed a new family of small molecule and ratiometric TP probes (BH series) for acidic pH. These benzimidazole derivatives, designed by a simple and flexible strategy, have pK_a values ranging from 4.9 to 6.1, and show a bright two-photon excited fluorescence. Their spectra are characterized by a marked blue-to-green emission color change in response to a decrease in pH from 7.5 to 4.0 and a distinctive isoemissive region. They exhibit easy loading and low cytotoxicity, thereby allowing quantitative analysis of acidic

dx.doi.org/10.1021/ja409971k | J. Am. Chem. Soc. 2013, 135, 17969−17977

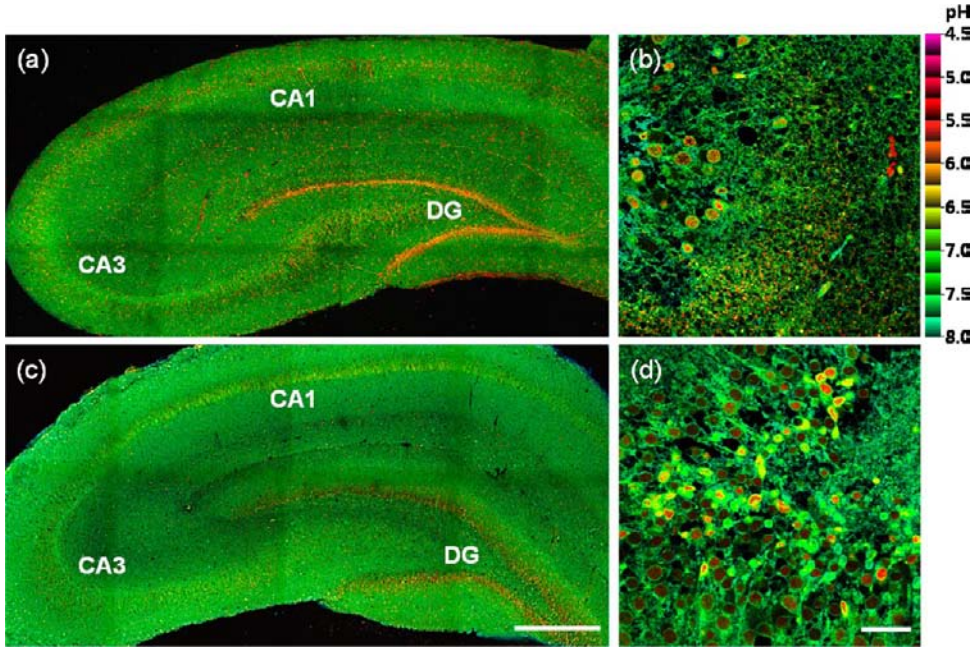

Figure 7. Pseudocolored ratiometric TPM images (I_{green}/I_{IR}) of a rat hippocampal slice stained with 30 μM (a and b) BH1L and (c and d) BH1. (a and c) 120 TPM images along the z-direction at the depths of approximately 90−180 μm were accumulated to visualize the overall pH distribution with 10× magnification. (b and d) Higher magnification images (63×) at the regions of DG. Excitation wavelength is 740 nm. Scale bars are (a and c) 300 μm and (b and d) 47 μm.

pH. Moreover, ratiometric TPM imaging revealed that BH1L allows for direct, real-time estimation of the pH values inside lysosomal compartments in live cells as well as in living mouse brain tissues. These findings demonstrate that these probes will find useful applications in biomedical research.

EXPERIMENTAL SECTION

Spectroscopic Measurements. Absorption spectra were recorded on a S-3100 UV−vis spectrophotometer and fluorescence spectra were obtained with FluoroMate FS-2 fluorescence spectrophotometer with a 1 cm standard quartz cell. The fluorescence quantum yield was determined by using 9,10-diphenylanthracene (Φ = 0.93 in cyclohexane) as the reference by the literature method.[21]

pK_a Value. A 3.0 μL of the stock solution of probe in DMSO (1.0×10^{-3} M) was added to a cuvette containing 3.0 mL of universal buffer solution by using a micro syringe to prepare 1.0 μM of probe solution and the spectral changes in the fluorescence were measured as a function of the pH (3.5−10.0). pK_a values of BH1−3 and BH1L were calculated by linear regression analysis of the fluorescence data to fit eq 1.

$$\mathrm{pH} = \mathrm{p}K_a + c\left[\log\frac{R - R_{min}}{R_{max} - R}\right] + \log\frac{I^a}{I^b} \quad (1)$$

where R is the observed ratios (I_{green}/I_{iso}) at isoemission point (I_{iso}) and 500−550 nm (I_{green}) at a given pH. R_{max} and R_{min} are maximum and minimum limiting value of R, respectively, and c is the slope.[22] I^a/I^b is the ratio of the fluorescent intensity in acid (pH 3.5) to the intensity in base (pH 10.0) at the wavelength chosen for the denominator of R. In this case, this correction vanishes by using the sharp isoemission point. To determine the pK_a^{TP} in a two-photon mode, the TPEF spectra were obtained by a CCD detector (Monora 320 spectrograph set with Andor iDus DV401A-BV). They were excited by a mode-locked titanium-sapphire laser source (Mai Tai HP, Spectra Physics, 80 MHz pulse frequency, 100 fs pulse width) set at wavelength 740 nm and output power 2510 mW, which corresponded to approximately 200 mW average power in the focal plane.

Measurement of Two-Photon Cross Section. The two-photon cross section (δ) was determined by using femtosecond (fs) fluorescence measurement technique as described.[23] Probe (1.0×10^{-6} M) was dissolved in universal buffer solutions at pH = 3.5, 7.2 and 10, respectively, and the two-photon induced fluorescence intensity was measured at 720−880 nm by using rhodamine 6G as the reference, whose two-photon property has been well characterized in the literature.[24] The intensities of the two-photon induced fluorescence spectra of the reference and sample emitted at the same excitation wavelength were determined. The TPA cross section was calculated by using $\delta = \delta_r(S_s\Phi_r\phi_r c_r)/(S_r\Phi_s\phi_s c_s)$, where the subscripts s and r stand for the sample and reference molecules. The intensity of the signal collected by a CCD detector was denoted as S. Φ is the fluorescence quantum yield. ϕ is the overall fluorescence collection efficiency of the experimental apparatus. The number density of the molecules in solution was denoted as c. δ_r is the TPA cross section of the reference molecule.

Cell Culture. HeLa human cervical carcinoma cells (ATCC, Manassas, VA, USA) were cultured in DMEM (WelGene, Inc., Seoul, Korea) supplemented with 10% FBS (WelGene), penicillin (100 units/mL), and streptomycin (100 μg/mL). Two days before imaging, the cells were passed and plated on glass-bottomed dishes (NEST). All the cells were maintained in a humidified atmosphere of 5/95 (v/v) of CO_2/air at 37 °C. For labeling, the growth medium was removed and changed with serum-free DMEM. The cells were treated and incubated with 3.0 μM probe at 37 °C under 5% CO_2 for 30 min.

Two-Photon Fluorescence Microscopy. Two-photon fluorescence microscopy images of probe-labeled cells and tissues were obtained with spectral confocal and multiphoton microscopes (Leica TCS SP8MP) with ×10 dry, ×40 oil, × 63 oil, and ×100 oil objectives, numerical aperture (NA) = 0.30, 1.30, 1.40, and 1.30, respectively. The two-photon fluorescence microscopy images were obtained with a DMI6000B Microscope (Leica) by exciting the probes with a mode-locked titanium-sapphire laser source (Mai Tai HP; Spectra Physics, 80 MHz pulse frequency, 100 fs pulse width) set at wavelength 740 nm and output power 2510 mW, which corresponded to approximately 10 mW average power in the focal plane. To obtain images at 440−460 nm (IR) and 500−550 nm (green) range, internal PMTs were used to collect the signals in an 8 bit unsigned 512 × 512 and 1024 × 1024 pixels at 400 and 200 Hz scan speed, respectively.

dx.doi.org/10.1021/ja409971k | J. Am. Chem. Soc. 2013, 135, 17969−17977

Ratiometric image processing and analysis was carried out using MetaMorph software.

Cell Calibration. A pH calibration curve was generated by I_{green}/I_{IR} of ionophore-treated and BH1- or BH1L-labeled HeLa cells. The cells were treated and incubated with 3.0 μL of 1 mM BH1 or 1 mM BH1L in DMSO stock solution (3.0 μM BH1 and 3.0 μM BH1L) at 37 °C under 5% CO_2 for 30 min, and then the extracellular media was replaced with 1 mL of calibration buffer (125 mM KCl, 20 mM NaCl, 0.5 mM $CaCl_2$, 0.5 mM $MgCl_2$, 5 μM nigericin, 5 μM monensin, and 25 mM buffer; acetate for pH 3.5, 4.0, 4.3, 5.0, 5.2; MES for pH 5.5, 6.0; HEPES for pH 6.5, 7.0, 8.0).[6e] The cells were treated with the calibration buffer for 15−20 min at room temperature. The TPEF intensity at 440−460 nm (I_{IR}) and 500−550 nm (I_{green}) of BH1 or BH1L is well changed with pH, and we obtained pH calibration curve by the plots of I_{green}/I_{IR} versus pH value.

Photostability. Photostability of BH1−3 and BH1L was determined by monitoring the changes in TPEF intensity with time at three designated positions of probe-labeled HeLa cells chosen without bias (Figure S5). The TPEF intensity remained nearly the same for 1 h, indicating their high photostability.

Cell Viability. To confirm that the probe could not affect the viability of HeLa cells in our incubation condition, we used MTS assay (Cell Titer 96H; Promega, Madison, WI, USA) according to the manufacture's protocol. The results are shown in Figure 3.

Preparation and Staining of Fresh Rat Hippocampal Slices. Slices were prepared from the hippocampi of 2-weeks-old rat (SD). Coronal slices were cut into 400 μm thickness using a vibrating-blade microtome in artificial cerebrospinal fluid (ACSF; 138.6 mM NaCl, 3.5 mM KCl, 21 mM $NaHCO_3$, 0.6 mM NaH_2PO_4, 9.9 mM D-glucose, 1 mM $CaCl_2$, and 3 mM $MgCl_2$). Slices were incubated with 30 μL of 10 mM stock solution of BH1 and BH1L in DMSO (total 30 μM BH1 and 30 μM BH1L) in ACSF bubbled with 95% O_2 and 5% CO_2 for 1 h at 37 °C. Slices were then washed three times with ACSF and transferred to glass-bottomed dishes (NEST) and observed in a spectral confocal multiphoton microscope. The TPM images were obtained at about 90−180 μm depth.

■ ASSOCIATED CONTENT

Supporting Information

Synthesis, additional methods, figures (Figure S1−S12) and table S1. This material is available free of charge via the Internet at http://pubs.acs.org.

■ AUTHOR INFORMATION

Corresponding Author

kimhm@ajou.ac.kr

Author Contributions

†H.J.K. and C.H.H. contributed equally.

Notes

The authors declare no competing financial interest.

■ ACKNOWLEDGMENTS

This work was supported by National Research Foundation (NRF) grants funded by the Korean Government (2011-0028663) and Priority Research Centers Program through the NRF (2009-0093826).

■ REFERENCES

(1) (a) Casey, J. R.; Grinstein, S.; Orlowski, J. *Nat. Rev. Mol. Cell Biol.* **2010**, *11*, 50. (b) Mellman, I.; Fuchs, R.; Helenius, A. *Annu. Rev. Biochem.* **1986**, *55*, 663. (c) Martinez-Zaguilan, R.; Seftor, E. A.; Seftor, R. E.; Chu, Y. W.; Gillies, R. J.; Hendrix, M. J. *Clin. Exp. Metastasis* **1996**, *14*, 176.

(2) (a) Kornfeld, S.; Mellman, I. *Annu. Rev. Cell Biol.* **1989**, *5*, 483. (b) Blott, E. J.; Griffiths, G. M. *Nat. Rev. Mol. Cell Biol.* **2002**, *3*, 122. (c) Stinchcombe, J.; Bossi, G.; Griffiths, G. M. *Science* **2004**, *305*, 55.

(3) Schindler, M.; Grabski, S.; Hoff, E.; Simon, S. M. *Biochemistry* **1996**, *35*, 2811.

(4) de Silva, A. P.; Gunaratne, H. Q.; Gunnlaugsson, T.; Huxley, A. J.; McCoy, C. P.; Rademacher, J. T.; Rice, T. E. *Chem. Rev.* **1997**, *97*, 1515.

(5) (a) Han, J.; Burgess, K. *Chem. Rev.* **2010**, *110*, 2709. (b) Hauglang, P. R. *The Handbook: A Guide to Fluorescent Probes and Labeling Technologies*, 10th ed.; Molecular Probes: Eugene, OR, 2005.

(6) (a) Whitaker, J. E.; Haugland, R. P.; Prendergast, F. G. *Anal. Biochem.* **1991**, *194*, 330. (b) Diwu, Z.; Chen, C. S.; Zhang, C.; Klaubert, D. H.; Haugland, R. P. *Chem. Biol.* **1999**, *6*, 411. (c) Galindo, F.; Burguete, M. I.; Vigara, L.; Luis, S. V.; Kabir, N.; Gavrilovic, J.; Russell, D. A. *Angew. Chem., Int. Ed.* **2005**, *44*, 6504. (d) Urano, Y.; Asanuma, D.; Hama, Y.; Koyama, Y.; Barrett, T.; Kamiya, M.; Nagano, T.; Watanabe, T.; Hasegawa, A.; Choyke, P. L.; Kobayashi, H. *Nat. Med.* **2009**, *15*, 104. (e) Lee, M.; Gubernator, N. G.; Sulzer, D.; Sames, D. *J. Am. Chem. Soc.* **2010**, *132*, 8828. (f) Myochin, T.; Kiyose, K.; Hanaoka, K.; Kojima, H.; Terai, T.; Nagano, T. *J. Am. Chem. Soc.* **2011**, *133*, 3401. (g) Chen, S.; Hong, Y.; Liu, Y.; Liu, J.; Leung, C. W. T.; Li, M.; Kwok, R. T. K.; Zhao, E.; Lam, J. W. Y.; Yu, Y.; Tang, B. Z. *J. Am. Chem. Soc.* **2013**, *135*, 4926.

(7) (a) Miesenbock, G.; De Angelis, D. A.; Rothman, J. E. *Nature* **1998**, *394*, 192. (b) Bizzarri, R.; Serresi, M.; Luin, S.; Beltram, F. *Anal. Bioanal. Chem.* **2009**, *393*, 1107.

(8) Yang, M.; Song, Y.; Zhang, M.; Lin, S.; Hao, Z.; Liang, Y.; Zhang, D.; Chen, P. R. *Angew. Chem., Int. Ed.* **2012**, *51*, 7674.

(9) (a) Helmchen, F.; Denk, W. *Nat. Methods* **2005**, *2*, 932. (b) Zipfel, W. R.; Williams, R. M.; Webb, W. W. *Nat. Biotechnol.* **2003**, *21*, 1369.

(10) (a) Kim, H. M.; Cho, B. R. *Acc. Chem. Res.* **2009**, *42*, 863. (b) Kim, H. M.; Cho, B. R. *Chem. Asian J.* **2011**, *6*, 58. (c) Sumalekshmy, C.; Fahrmi, C. J. *Chem. Mater.* **2011**, *23*, 483. (d) Yao, S.; Belfield, K. D. *Eur. J. Org. Chem.* **2012**, 3199.

(11) Yao, S.; Schafer-Hales, K. J.; Belfield, K. D. *Org. Lett.* **2007**, *9*, 5645.

(12) Park, H. J.; Lim, C. S.; Kim, E. S.; Han, J. H.; Lee, T. H.; Chun, H. J.; Cho, B. R. *Angew. Chem., Int. Ed.* **2012**, *51*, 2673.

(13) Srivastava, J.; Barber, D. L.; Jacobson, M. P. *Physiology* **2007**, *22*, 30.

(14) Lide, D. R. *The Handbook of Chemistry and Physics*, 89th ed.; CRC Press: Boca Raton, FL, 2008.

(15) (a) Masanta, G.; Lim, C. S.; Kim, H. J.; Han, J. H.; Kim, H. M.; Cho, B. R. *J. Am. Chem. Soc.* **2011**, *133*, 5698. (b) Heo, C. H.; Kim, K. H.; Kim, H. J.; Baik, S. H.; Song, H.; Kim, Y. S.; Lee, J.; Mook-Jung, I.; Kim, H. M. *Chem. Commun.* **2013**, *49*, 1303.

(16) Kim, H. M.; An, M. J.; Hong, J. H.; Jeong, B. H.; Kwon, O.; Hyon, J. Y.; Hong, S. C.; Lee, K. J.; Cho, B. R. *Angew. Chem., Int. Ed.* **2008**, *47*, 2231.

(17) Charier, S.; Ruel, O.; Baudin, J. B.; Alcor, D.; Allemand, J. F.; Meglio, A.; Jullien, L. *Angew. Chem., Int. Ed.* **2004**, *43*, 4785.

(18) (a) Kim, H. M.; Cho, B. R. *Chem Commun.* **2009**, 153. (b) Sumalekshmy, S.; Henary, M. M.; Siegel, N.; Lawson, P. V.; Wu, Y.; Schmidt, K.; Bredas, J. L.; Perry, J. W.; Fahrni, C. J. *J. Am. Chem. Soc.* **2007**, *129*, 11888.

(19) Ohkuma, S.; Poole, B. *Proc. Natl. Acad. Sci. U.S.A.* **1978**, *75*, 3327.

(20) (a) van Praag, H.; Schinder, A. F.; Christie, B. R.; Toni, N.; Palmer, T. D.; Gage, F. H. *Nature* **2002**, *415*, 1030. (b) Kuhn, H. G.; Dickinson-Anson, H.; Gage, F. H. *J. Neurosci.* **1996**, *16*, 2027. (c) Datson, N. A.; Morsink, M. C.; Steenbergen, P. J.; Aubert, Y.; Schlumbohm, C.; Fuchs, E.; de Kloet, E. R. *Hippocampus* **2009**, *19*, 739.

(21) (a) Demas, J. N.; Crosby, G. A. *J. Phys. Chem.* **1971**, *75*, 991. (b) Brouwer, A. M. *Pure Appl. Chem.* **2011**, *83*, 2213.

(22) (a) Myochin, T.; Kiyose, K.; Hanaoka, K.; Kojima, H.; Terai, T.; Nagano, T. *J. Am. Chem. Soc.* **2011**, *133*, 3401. (b) Whitaker, J. E.; Haugland, R. P.; Prendergast, F. G. *Anal. Biochem.* **1991**, *194*, 330.

(23) Lee, S. K.; Yang, W. J.; Choi, J. J.; Kim, C. H.; Jeon, S.-J.; Cho, B. R. *Org. Lett.* **2005**, *7*, 323.
(24) Makarov, N. S.; Drobizhev, M.; Rebane, A. *Opt. Express* **2008**, *6*, 4029.